The background of the slide is a large, pixelated heatmap. It features a color gradient from dark blue at the bottom to bright yellow at the top, with various shades of cyan and orange in between, creating a noisy, abstract pattern.

Effect of non-adiabatic electron dynamics on turbulent transport in fusion plasmas

Ajay C.J.

Presentation at
PPPL, Princeton

29 April 2021

■ Introduction

- ▶ Microturbulence in the tokamak core

■ **How eigenmode self-interaction affects zonal flows**

[Ajay C.J. et. al., JPP 86, 905860504 (2020)]

1. Zonal flow driving mechanisms:

- ▶ Modulational instability, MI
- ▶ Self-interaction, SI

2. Non-adiabatic electron response in ITG eigenmodes

3. Evidence of zonal flow drive by MI and SI in turbulence simulations

- ▶ Non-adiabatic electron response amplifies SI

4. A system size effect resulting from SI

■ **Effect of collisions on non-adiabatic electron response**

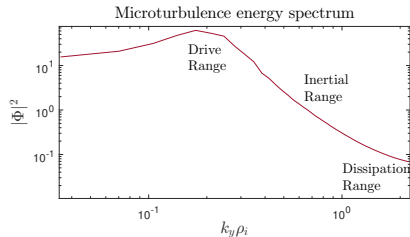
[Ajay C.J. et. al., *submitted to POP*, arXiv:2104.12585 (2021)]

■ **δT_e measurement in TCV and verification with gyrokinetic simulations**

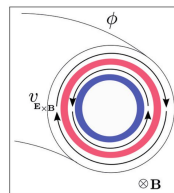
[M. Fontana et al., NF 60, 016006 (2019)]

■ Summary

- Equilibrium pressure gradient can give rise to micro-instabilities
 - Turbulent transport of heat and particles
 - Loss of confinement
- Common microinstabilities in present day tokamaks
 1. Ion Temperature Gradient (ITG)
 2. Trapped Electron Mode (TEM)
 3. Electron Temperature Gradient (ETG), and more
- Turbulence saturation
 1. Zonal flows
 2. Collisions
 3. Damped eigenmodes, and more
- Gyrokinetic codes are used to simulate turbulence
 - GENE code [F. Jenko, et al., Phys. Plasmas 7, 1904 (2000)]
- Field aligned coordinate system:
 - $x = \text{fct}(\psi)$: radial
 - $y = \frac{r_0}{q_0} [q(\psi)\chi - \varphi]$: binormal
 - $z = \chi$: parallel
 - (ψ, χ, φ) : straight field line magnetic coordinates



Zonal flow shearing



[G. Merlo, PhD Thesis (2016)]

Zonal flow driving mechanisms

Modulational Instability

In a Shearless Slab:

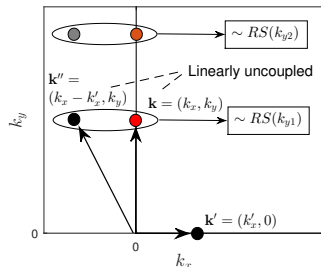
Eigenmodes = Fourier modes $\mathbf{k} = (k_x, k_y)$.

- Resonant decay mechanism** $\mathbf{k} \rightarrow \mathbf{k}', \mathbf{k}''$ involving 3 linearly decoupled modes with $\mathbf{k} = \mathbf{k}' + \mathbf{k}''$ and **frequency matching** $\omega_{\mathbf{k}} \simeq \omega_{\mathbf{k}'} + \omega_{\mathbf{k}''}$.

[A. Hasegawa, et al., Phys. Fluids 22, p2122 (1979)]

- Modulational Instability (MI)** = two coupled resonant interactions: $\mathbf{k} \rightarrow \mp \mathbf{k}', \mathbf{k}_{\pm}; \mathbf{k}_{\pm} = \mathbf{k} \pm \mathbf{k}'$.

\Rightarrow A finite amplitude zonal mode \mathbf{k}' can stimulate the **coherent decay** of multiple \mathbf{k} modes.



Self-interaction

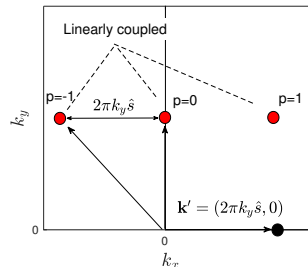
In a Sheared Torus:

Eigenmodes of the form:

$$\Phi(x, y, z) = e^{ik_y y} \sum_{p=-\infty}^{\infty} \hat{\Phi}_{k_x, k_y}(z) e^{ik_x x} \\ k_x = k_{x0} + p2\pi k_y \hat{s}$$

- Self-Interaction (SI):** Fixed relative phases between the linearly coupled Fourier modes $k_x = k_{x0} + p2\pi k_y \hat{s} \Rightarrow$ zonal modes ($p2\pi k_y \hat{s}, k_y = 0$) driven with **fixed phases**

\Rightarrow stationary $\omega_{E \times B}$ structures localized at MRSs $x = p/k_y \hat{s}$.



- Adiabatic electron response: $n_e(\mathbf{x}) = N(x)e^{e\Phi(\mathbf{x})/T_{0,e}(x)}$

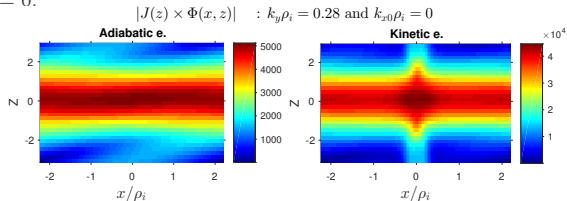
Adiabatic condition $|\omega/k_{||}| \ll v_{th,e}$.

Violated at MRS where $k_{||} \approx (nq + m)/Rq = 0$.

- Non-adiabatic passing electron response

⇒ **Fine structures at Mode Rational Surface (MRS).**

[J.Dominski, et al., Phys.Plasmas 22, 062303(2015)]

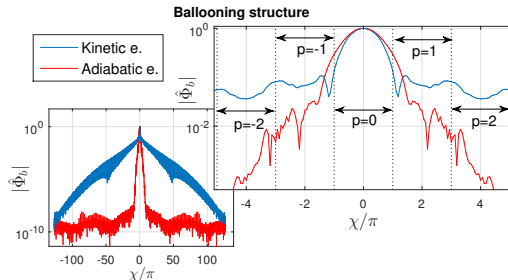


- An eigenmode takes the form:

$$\Phi(x, y, z) = e^{ik_y y} \sum_{\substack{p=-\infty \\ k_x = k_{x0} + p2\pi k_y \hat{s}}}^{\infty} \hat{\Phi}_{k_x, k_y}(z) e^{ik_x x}$$

Parallel boundary condition:

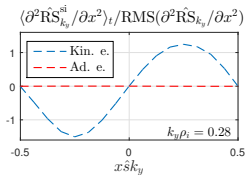
$$\hat{\Phi}_{k_x, k_y}(z + 2\pi) = \hat{\Phi}_{k_x + 2\pi k_y \hat{s}, k_y}(z)$$



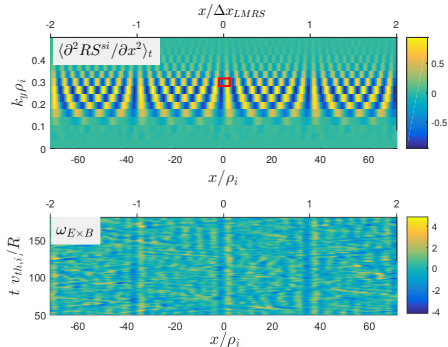
- $RS \simeq \langle \tilde{V}_{E \times B, x} \tilde{V}_{E \times B, y} \rangle_{y, z}$ can be considered as a proxy to the drive of zonal flows: $\frac{\partial}{\partial t} \omega_{E \times B} \sim \frac{\partial^2}{\partial x^2} RS$
- SI contribution to Reynolds stress $\hat{RS}_{k_y}(x)$ given by:

$$\hat{RS}_{k_y}^{SI}(x) = \text{Real} \sum_{k_{x1}} \sum_{\substack{p=-\infty \\ k_{x2}=k_{x1}+p2\pi k_y \hat{s}}}^{\infty} \left\langle \frac{2}{B_0^2} \left(k_{x1} k_y g^{xx} + k_y^2 g^{xy} \right) \hat{\Phi}_{k_{x1} k_y}^* \hat{\Phi}_{k_{x2} k_y} \right\rangle_z e^{i(k_{x2}-k_{x1})x}$$

- With kinetic electrons, self-interaction part of Reynolds Stress remains persistent (with same phase) and dominant.



- Time-averaged contributions to $\partial^2 RS^{si} / \partial x^2$ from different k_y s aligned near Low(est) order MRSs \Rightarrow non-zero $\langle \omega_{E \times B} \rangle_t$ structures.
- Away from LMRs, time-averaged contributions from different k_y s cancel $\Rightarrow \langle \omega_{E \times B} \rangle_t \simeq 0$. But, fluctuating contributions are present everywhere in $x \Rightarrow SD_{x,t}(\omega_{E \times B}) \neq 0$.



- **Bicoherence analysis** measures level of phase matching in 3 Fourier mode interactions, characteristic of MI.

- Bicoherence for Fourier mode triplet $(\mathbf{k}, \mathbf{k}', \mathbf{k}'')$, such that $\mathbf{k} = \mathbf{k}' + \mathbf{k}''$, is defined here as:

$$b(\mathbf{k}; \mathbf{k}') = \frac{|\langle \hat{\Phi}_{\mathbf{k}}^* \hat{\Phi}_{\mathbf{k}'} \hat{\Phi}_{\mathbf{k}''} \rangle_t|}{\langle |\hat{\Phi}_{\mathbf{k}}^* \hat{\Phi}_{\mathbf{k}'} \hat{\Phi}_{\mathbf{k}''}| \rangle_t}$$

$$B(\mathbf{k}; \mathbf{k}') = \frac{b(\mathbf{k}; +\mathbf{k}') + b(\mathbf{k}; -\mathbf{k}')}{2}$$

⇒ **Adiabatic electrons:** Coherent (and thus correlated) contributions from different $k_y \neq 0$ modes to drive of a given zonal mode. Evidence of strong MI.

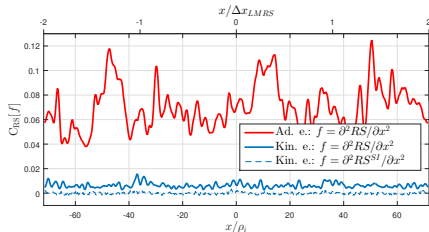
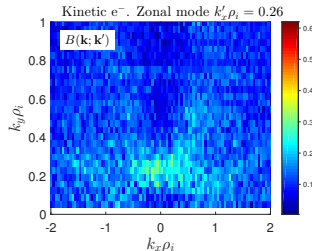
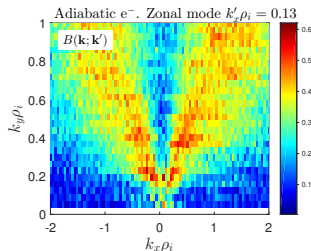
⇒ **Kinetic electrons:** Less coherent contributions to drive of zonal modes. MI mechanism is weakened.

- Considering average correlation estimate:

$$C_{RS}[f] = \sum_{\substack{k_{y,i}, k_{y,j} \\ k_{y,j} > k_{y,i}}} \frac{\text{Cov}[\hat{f}_{k_{y,i}}, \hat{f}_{k_{y,j}}]}{\sigma[\hat{f}_{k_{y,i}}] \sigma[\hat{f}_{k_{y,j}}]} / \sum_{\substack{k_{y,i}, k_{y,j} \\ k_{y,j} > k_{y,i}}} 1$$

- Contributions from SI are fully decorrelated, reflecting that they essentially act as **independent random kicks** when driving ZFs.

$B(\mathbf{k}; \mathbf{k}')$ as a function of $\mathbf{k} = (k_x, k_y)$ for given zonal mode $\mathbf{k}' = (k'_x, 0)$.



A system size effect resulting from SI

Significance of fluctuating zonal flows

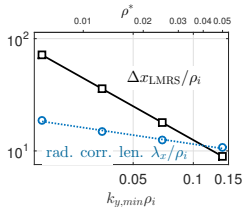
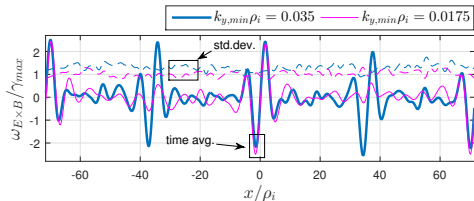
■ $k_{y,\min}\rho_i = (n_{\min}q_0 a/r_0)\rho^*$, with $\rho^* = \rho_i/a$

⇒ scan in $k_{y,\min}\rho_i$ addresses a particular system size effect.

■ As $k_{y,\min} \rightarrow 0$

⇒ distance $\Delta x_{LMRS} = 1/k_{y,\min}\hat{s}$ between LMRs where $\langle\omega_{E\times B}\rangle_t \neq 0$ increases

⇒ Higher fluxes ?... Not the full picture!

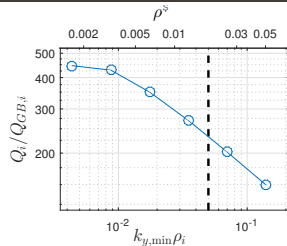


■ As $k_{y,\min}\rho_i \rightarrow 0$, the radial extent λ_x of turbulent eddies becomes smaller than Δx_{LMRS} .

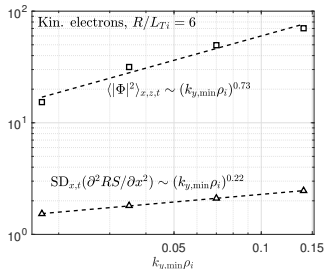
⇒ *Fluctuating component* of ZFs are actively shearing turbulent eddies *in between* LMRs.

■ SI explains the system size effect:

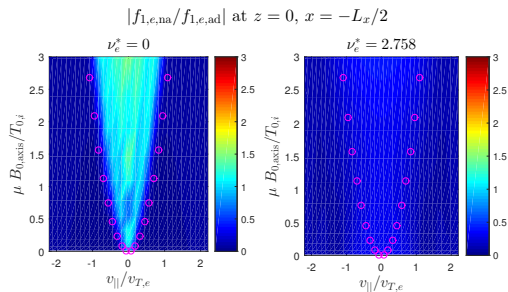
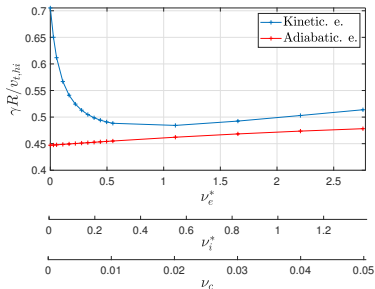
Using a statistical scaling argument, one gets,
 $SD_{x,t}(\partial^2 RS/\partial x^2) \sim (k_{y,\min}\rho_i)^{0.23}$.



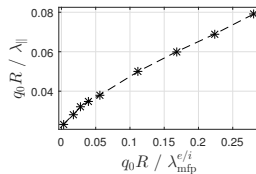
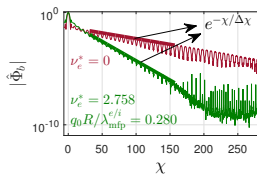
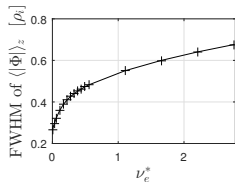
[J. Ball et al., JPP 86, 905860207 (2020)]



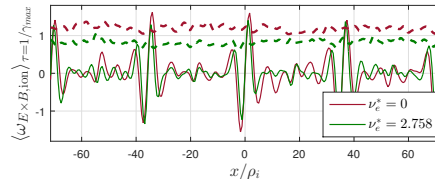
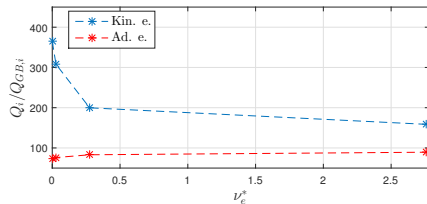
- With increasing collisionality, growth rate decreases [D. Mikkelsen et al., PRL 101, 135003 (2008)]
- Increased trapped-detrapped electron mixing → Increased adiabatic-like electron response



- Increase in radial width of fine-structures \iff parallel length scale ($\lambda_{||} = R q_0 \Delta \chi$) associated with the tail of the ballooning structure scales with electron-ion mean free path.

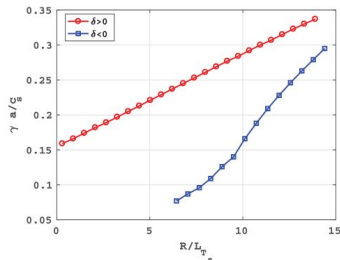
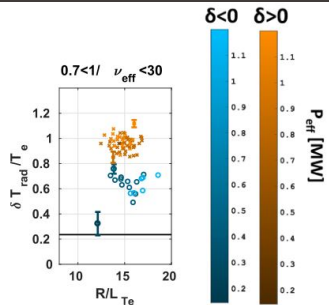


- Heat flux decreases with increasing collisionality.
 - ▶ A result of corresponding decrease in linear growth rate
→ Verified by a quasi-linear and zonal flow shearing rate analysis
- Stationary fine structures remain significant with respect to their fluctuation levels.
- Self-interaction measured by $\langle \partial^2 RS^{si} / \partial x^2 \rangle_t / \text{RMS}(\partial^2 RS / \partial x^2)$ for a single k_y
→ increases with increasing collisionality.
- Combined effect of self-interaction measured by the bicoherence and correlation analysis for multiple k_y s simultaneously
→ decreases with increasing collisionality.
- Greater the number of k_y modes contributing significantly to turbulence
→ more the decorrelated drive from multiple k_y s.
- Parallel with increasing collisionality and decreasing $R/L_{T,i}$
→ bicoherence and correlation levels indeed increases as one moves closer to marginal stability.



[M. Fontana et al., Nuclear Fusion, 60, 016006 (2019)]

- Increased confinement in negative triangularity plasmas compared to positive triangularity.
[Z. Huang et al., PPCF 61 014021 (2018)]
[M. Fontana et al., NF 58 024002(2017)]
- Electron temperature fluctuations measured using Correlation Electron Cyclotron Emission (CECE) diagnostic.
- Extending electron temperature measurements to NBI heated plasmas with $T_e/T_i \sim 1$.
- Lower growth rate and higher critical gradients observed in linear GENE sims for negative triangularity.



- Non-adiabatic electron response amplifies zonal flow drive via the self-interaction mechanism.
- Self-interaction Reynolds stress contribution from each toroidal mode is uncorrelated with each-other, disrupts modulational instability mechanism, and can lead to a system size effect.
- Collisions affect non-adiabatic electron response and the self-interaction mechanism
- Experiment-gyrokinetic verification of improved confinement in negative δ plasma for $T_e/T_i \sim 1$ in TCV.
- A few additional comments:
 - ▶ Background flow shear study with non-adiabatic electrons similar to that with adiabatic electrons.
 - ▶ Attempt to measure the fine-structures at low order MRSs in TCV.

Thanks!